sciendo

PRODUCTION ENGINEERING ARCHIVES 25 (2019) 1-7

PRODUCTION ENGINEERING ARCHIVES

ISSN 2353-5156 (print)
ISSN 2353-7779 (online)

Exist since 4th quarter 2013
Available online at www.pea-journal.eu

Mathematical and experimental study of deformations of a steel roll of a road roller with a variable geometry of a contact surface

Mikhail Doudkin[1], Alina Kim[1], Murat Sakimov[1]

[1] East Kazakhstan State Technical University, Ust-Kamenogorsk, Kazakhstan, e-mail: doudkin@mail.ru

Article history
Received 09.09.2019
Accepted 20.10.2019
Available online 09.12.2019

Keywords
shell
road roller
drum
steel
stress

Abstract
The lack of a common methodology on compaction theory stimulates developers of road construction equipment to create various approximate methods for their calculation, the number of which, at the present time, is comparable with the nomenclature of the proposed designs of rollers. The article presents the analysis of the deformable shell behavior of a road roller, and the compacted material under its compacting roller, in a situation when a rigid circular shell of the roller is replaced by a forcefully deformable elliptical shape, which, unlike the circular design, allows variation, adjustment and optimization of the road roller impact on the material to be compacted.

DOI: 10.30657/pea.2019.25.01 JEL: L69, M11:

1. Introduction

The mathematical interpretation of the stress-strain state of a cylindrical shell element using differential equations, considered in previous studies (Dudkin et al., 2006; Abdeev et al., 2011; Sakimov et al., 2018), is an approximate one, since it is based on a flat-plate model having an initial death. This simplifying assumption did not allow, with sufficient objectivity and reliability, to quantify the possible stability loss of the shell in the local area of its contact with the road surface material to be compacted. This assertion-assumption is legitimate from the point of view of the almost complete analogy of the deformation shell of a double-hinged arch under the action of a uniformly distributed load $q = const$, where, even in the linear formulation of the problem, the upper level of the critical pressure q_{kv} is determined (Kolkunov, 1972).

Therefore, it is necessary to clarify the general conceptual approach adopted in the first part of this article by a nonlinear mechanical-mathematical model of an elastic gently sloping arched system under the conditions of its cylindrical bend using the curvilinear coordinate x_1 with a confirmed simplification about the constancy of the curvature of the curve, and also provided that the external loads $q_{\text{p}} = q_{\text{p}}(x_1)$ and deflection $\omega = \omega(x_1)$, there are directed along the normal to the initial surface (Fig. 1) $y_1(x_1)$.

2. Mechanical-mathematical model

Considering the nature of the pressure function $q_{\text{p}}(x_1)$ and the fixing scheme of the element shown in Fig. 1 should be considered that the subcritical compressive stress σ_{ox} corresponds to the main moment state of the shell (Fig. 2), in which it is necessary to take into account the bending forces (Kolkunov, 1972). For this purpose, a fictitious transverse radial load is introduced, as in the linear theory instead of the force parameter q_{p}.

$$q_{\text{p}} = q_{\text{p}}(x_1) = -\delta \cdot \sigma_{ox} \cdot \frac{d^2\omega}{dx_1^2}, \tag{1}$$

equivalent to the action of stress σ_{ox} and equal to the projection of the distributed force σ_ox to the direction of the normal to the curved surface (Fig. 1). From equilibrium condition (Kolkunov, 1972):

$$\sigma_{ox} = \sigma_{ox}(x_1) = \left[\frac{q_p}{\delta} - \frac{E \cdot \delta^2}{12(1-\mu^2)} \cdot \frac{d^4\omega}{dx_1^4}\right] \cdot \frac{a^2}{b} =$$

$$= \left[\frac{q}{l_p \cdot \delta}\sqrt{l_p^2 - x_1^2} - \frac{E \cdot \delta^2}{12(1-\mu^2)} \cdot \frac{d^4\omega}{dx_1^4}\right] \cdot \frac{\pi R_c}{2 \cdot E(\xi)\sqrt{1-\xi^2}}. \tag{2}$$

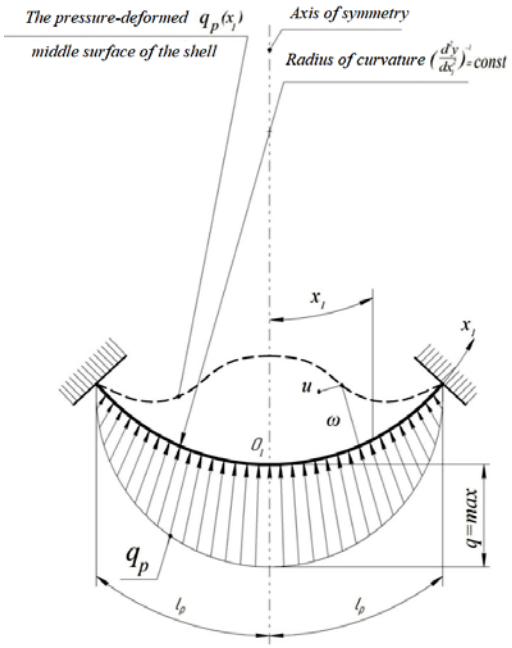

Fig. 1. Refined theoretical design model of the shell element in the form of a flat cylindrical shell-arch (Kolkunov, 1972) to assess its local stability

Replacing $q_p = \frac{q}{l_p}\sqrt{l_p^2 - x_1^2} = q\sqrt{1-\frac{x_1^2}{l_p^2}}$ according to (1), (2), a refined-transformed nonlinear differential equation is obtained

$$\frac{E\cdot\delta^2}{12(1-\mu^2)}\cdot\frac{d^4\omega}{dx_1^4} - A\left(\frac{d^2\omega}{dx_1^2} + \frac{2\cdot E(\xi)\sqrt{1-\xi^2}}{\pi R_c}\right) + \\ + \frac{q}{\delta}\sqrt{1-\frac{x_1^2}{l_p^2}}\cdot\frac{\pi R_c}{2\cdot E(\xi)\sqrt{1-\xi^2}}\cdot\frac{d^2\omega}{dx_1^2} - \\ - \frac{E\cdot\delta^2}{12(1-\mu^2)}\cdot\frac{d^4\omega}{dx_1^4}\cdot\frac{d^2\omega}{dx_1^2}\cdot\frac{\pi R_c}{2\cdot E(\xi)\sqrt{1-\xi^2}} = 0, \quad (3)$$

where the constant A is found using the same method, but using the relative deformation formula $\varepsilon_{x_1} = \varepsilon_{x_1}(x_1)$ with curvilinear coordinate x_1 when counting the movement $u(x_1)$ parallel to the arc l_p (Fig. 1), that is:

$$\varepsilon_{x_1} = \frac{du}{dx_1} - \frac{d^2y_1}{dx_1^2}\omega + \frac{1}{2}\left(\frac{d\omega}{dx_1}\right)^2 = \\ = \frac{du}{dx_1} - \frac{2\cdot E(\xi)\sqrt{1-\xi^2}}{\pi R_c}\omega + \frac{1}{2}\left(\frac{d\omega}{dx_1}\right)^2 = \frac{A}{E} \quad (4)$$

Whence, after substituting ω and performing the integration procedure, taking into account compliance with the kinematic boundary condition $u(\pm l_p) = 0$, the following is obtained:

$$u = u(x_1) = \int\left[\frac{A}{E} - \frac{1}{2}\left(\frac{d\omega}{dx_1}\right)^2 - \frac{2\cdot E(\xi)\sqrt{1-\xi^2}}{\pi R_c}\omega\right]dx_1 = \\ = \frac{A}{E}x_1 - 8f^2\left(\frac{x_1^3}{3l_p^4} - 2\frac{x_1^5}{5l_p^6} + \frac{x_1^7}{5l_p^8}\right) + \\ + \frac{2\cdot E(\xi)\sqrt{1-\xi^2}}{\pi R_c}\cdot f\cdot\left(x_1 - \frac{2x_1^3}{3l_p^2} + \frac{x_1^5}{5l_p^4}\right) + C. \quad (5)$$

Revealing obvious boundary equalities $u(0) = 0$ and $u(\pm l_p) = 0$, the result is (Fig. 1):

$$C = 0; A = \frac{16}{15}E\left(\frac{4}{7}\cdot\frac{f^2}{l_p^2} - \frac{2\cdot E(\xi)\sqrt{1-\xi^2}}{\pi R_c}\cdot f\right) \quad (6)$$

Equation (2) is solved using the Bubnov-Galerkin method (Birger et al., 1979; Bostanov et al., 2018; Temirbekov et al.,, 2019), using the already known values (6) and tables of type integrals (Doudkin et al., 2013):

$$2\int_0^{l_p}\nabla_\omega(x_1)\cdot\left(1 - \frac{2x_1^2}{l_p^2} + \frac{x_1^4}{l_p^4}\right)dx_1 = 0, \Rightarrow \quad (7)$$

$$\frac{E\cdot\delta^2}{12(1-\mu^2)}\cdot\frac{64f}{5l_p^3} - \left(\frac{16}{15}\right)^2\cdot\left(\frac{4f^2}{7l_p^2} - \frac{E(\xi)\sqrt{1-\xi^2}}{\pi R_c}f\right)\times \\ \times\left(-\frac{8f}{7l_p} + \frac{l_p E(\xi)\sqrt{1-\xi^2}}{\pi R_c}\right)E - \frac{25\pi\cdot f}{64\cdot\delta\cdot l_p}\cdot\frac{\pi R_c}{2E(\xi)\sqrt{1-\xi^2}}q + \\ + \frac{E\cdot\delta^2}{12(1-\mu^2)}\cdot\frac{24f^2}{l_p^4}\cdot\frac{128}{105l_p}\cdot\frac{\pi R_c}{2\cdot E(\xi)\sqrt{1-\xi^2}} = 0; \quad (8)$$

where $\nabla_\omega(x_1)$ – the left side of expression (2) in the form of a differential-algebraic operator and an additional definite integral (Doudkin et al., 2013)

$$\int_0^{l_p}\frac{d^2\omega}{dx_1^2}\sqrt{1-\frac{x_1^2}{l_p^2}}\cdot\left(1 - \frac{2x_1^2}{l_p^2} + \frac{x_1^4}{l_p^4}\right)dx_1 = \\ = 4f\int_0^{l_p}\left(-\frac{1}{l_p} + \frac{3x_1^2}{l_p^4}\right)\cdot\left(1 - \frac{2x_1^2}{l_p^2} + \frac{x_1^4}{l_p^4}\right)\sqrt{1-\frac{x_1^2}{l_p^2}}dx_1 = \\ = 4f\int_0^{l_p}\left(-\frac{1}{2l_p} + \frac{5}{8l_p} - \frac{7}{16l_p} + \frac{15}{4\cdot 32l_p}\right)arcsin\frac{x_1}{l_p}\Big|_0^{l_p} = -\frac{25\cdot\pi\cdot f}{64l_p} \quad (9)$$

After the term-by-term division of expression (8) into f and simple transformations, there is in a finite explicit form, the characteristic second – order functional dependence (Kolkunov, 1972) between q and f:

$$q = q(f) = \frac{2048}{375\pi}E\frac{\delta}{R_c}\left\{\frac{E(\xi)}{\pi}\sqrt{1-\xi^2}\left[\frac{\delta^2}{l_p^2(1-\mu^2)} + \right.\right. \\ \left. + \left(\frac{16}{15}\right)\cdot\left(\frac{32f^2}{49l_p^2} - \frac{12}{7}\cdot\frac{f}{R_c}\cdot\frac{E(\xi)}{\pi}\sqrt{1-\xi^2} + \left(\frac{E(\xi)}{\pi}\sqrt{1-\xi^2}\right)^2\frac{l_p^2}{R_c^2}\right)\right] + \\ \left. + \frac{24}{21(1-\mu^2)}\cdot\frac{\delta^3 f}{l_p^4}\right\} \quad (10)$$

At $f = 0$ from equality (10) the general design formula for the upper critical pressure q_{kv} (Kolkunov, 1972) is obtained

$$q_{kv} = \frac{2048}{375\pi}E\frac{\delta}{R_c}\times \\ \times\left[\frac{\delta^2}{l_p^2(1-\mu^2)} + \left(\frac{16}{15}\right)\frac{l_p^2}{R_c^2}\left(\frac{E(\xi)}{\pi}\sqrt{1-\xi^2}\right)^2\right]\frac{E(\xi)}{\pi}\sqrt{1-\xi^2}, \quad (11)$$

which (Abdeev et al., 2011) is for round ($\xi = 0$, $E(0) = 1{,}5708$) and elliptical ($\xi = \xi_p = 0{,}57, E(0{,}57) = 1{,}434$) shells is written as follows:

$$q_{kv}^{(к)} = \frac{1024}{375\pi}E\frac{\delta}{R_c}\left[\frac{\delta^2}{l_p^2(1-\mu^2)} + \left(\frac{4}{15}\right)\frac{l_p^2}{R_c^2}\right], \quad (12)$$

$$q_{kv}^{(E)} = \frac{2048}{375\pi}E\frac{\delta}{R_c}\left[\frac{\delta^2}{l_p^2(1-\mu^2)} + \left(\frac{16}{15}\right)\cdot 0{,}14066\cdot\frac{l_p^2}{R_c^2}\right]\cdot 0{,}37504 \quad (13)$$

Using the derived relations (12), (13), determine $q_{kv}^{(к)}$ і $q_{kv}^{(E)}$ at $l_{\text{p}} = 90\ mm,\ R_c = 600\ mm, \delta = 6{,}5\ mm,$ $\text{E} = 196000\ \left(\frac{N}{mm^2}\right),\ \mu = 0{,}256, \pi = 3{,}1416$:

$$q_{kv}^{(к)} = \frac{1024 \cdot 196000 \cdot 6{,}5}{375 \cdot 3{,}1416 \cdot 600} \cdot$$

$$\cdot \left\{ \left(\frac{6{,}5}{90}\right)^2 \cdot \frac{1}{[1-(0{,}256)^2]} + \left(\frac{4}{15}\right)\left(\frac{90}{600}\right)^2 \right\} = 21{,}37\ \frac{N}{mm^2}, \quad (14)$$

$$q_{kv}^{(E)} = \frac{2048 \cdot 196000 \cdot 6{,}5}{375 \cdot 3{,}1416 \cdot 600} \cdot$$

$$\cdot \left\{ \left(\frac{6{,}5}{90}\right)^2 \cdot \frac{1}{[1-(0{,}256)^2]} + \left(\frac{16}{15}\right) \cdot 0{,}14066 \cdot \left(\frac{90}{600}\right)^2 \right\} \cdot$$

$$\cdot\, 0{,}37504 = 12{,}4\ \frac{N}{mm^2} \quad (15)$$

The stability condition is observed with a large margin, as in accordance with the calculated data (14), (15).

$$\left.\begin{aligned} n_y^{(к)} &= \frac{q_{kv}^{(к)}}{q_{mp}^{(к)}} = \frac{21{,}37}{3{,}684} = 5{,}8 \gg [n_y] = 1{,}5 \\ n_y^{(E)} &= \frac{q_{kv}^{(E)}}{q_{mp}^{(E)}} = \frac{12{,}4}{4{,}727} = 2{,}62 \gg [n_y] = 1{,}5 \end{aligned}\right\} \quad (16)$$

Equating to zero the first derivative $\frac{dq}{df} = 0$ function, determine the maximum deflection f_n (Fig. 1):

$$f_n = \left(\frac{21}{16}\right) \cdot \frac{l_p^2}{R_c} \cdot \frac{E(\xi)}{\pi} \sqrt{1-\xi^2} -$$

$$- \frac{105}{(1-\mu^2)\cdot 128} \cdot \frac{\delta^3}{l_p^2} \cdot \frac{\pi}{E(\xi)\ \sqrt{1-\xi^2}}, \quad (17)$$

adequate lower practical load q_{kn} (Kolkunov, 1972), including (at $\pi = 3{,}1416$):

– for shell of circular profile ($\xi = 0,\ E(0) = 1{,}5708$)

$$n = \left(\frac{21}{16}\right) \cdot \frac{90^2}{600} \cdot \frac{1}{2} - \frac{105}{128} \cdot \frac{(6{,}5)^3 \cdot 2}{[1-(0{,}256)^2] \cdot 90^2} = 8{,}8\ mm \quad (18)$$

– for elliptical shell ($\xi = \xi_{\text{п}} = 0{,}57, E(0{,}57) = 1{,}434$)

$$f_{\text{н}}^{(E)} = \left(\frac{21}{16}\right) \cdot \frac{90^2 \cdot 1{,}434 \cdot 0{,}82164}{600 \cdot 3{,}1416} - \frac{105}{128} \times$$

$$\times \frac{(6{,}5)^3 \cdot 3{,}1416}{[1-(0{,}256)^2] \cdot 90^2 \cdot 1{,}434 \cdot 0{,}82164} = 6{,}58\ mm \quad (19)$$

The derived formulas (9) - (12), (17) are illustrated in Figure 2 of the existing classical curves (Kolkunov, 1972) (see Table 1)

Table 1. Values of the function (20) and (21) to the construction of the corresponding graphs presented in Fig. 2.

f, mm	0	2	4	6	8	10	12	14	16	18	20
$q^{(к)}, \frac{N}{mm^2}$	21,37	16,43	12,74	10,32	9,2	9,31	10,7	13,37	17,38	22,52	29
$q^{(э)}, \frac{N}{mm^2}$	12,4	9,74	8,04	7,29	7,49	8,64	10,74	13,8	17,8	22,76	28,67

$$q^{(к)} = q^{(к)}(f) =$$

$$= 3691{,}186(0{,}000043f^2 - 0{,}0007568f + 0{,}00579) \quad (20)$$

$$q^{(E)} = q^{(E)}(f) =$$

$$= 3691{,}186(0{,}0000322f^2 - 0{,}0004235f + 0{,}003356) \quad (21)$$

by analogy with the cubic dependencies of the simplified model. The graphs of the functional relations (20), (21), vividly characterizing the equilibrium state of the refined-modified mechanical system (Fig 1 and 2), along with the regular values of Table 1 contain special points including upper $q_{kv}^{(к)}, q_{kv}^{(E)}$ and bottom $q_{kn}^{(к)},\ q_{kn}^{(E)}$ extreme critical pressures:

$$\left.\begin{aligned} q_{kv}^{(к)} &= 21{,}37\ \frac{N}{mm^2}, q_{kv}^{(E)} = 12{,}4\ \frac{N}{mm^2}, \\ q_{kn}^{(к)} &= 9{,}08\ \frac{N}{mm^2}, q_{kn}^{(E)} = 7{,}22\ \frac{N}{mm^2}, \end{aligned}\right\} \quad (22)$$

as well as corresponding movements

$$\left.\begin{aligned} f_в^{(к)} &= f_в^{(э)} = 0, \\ f_n^{(к)} &= 8{,}8\ мм, f_n^{(E)} = 6{,}58\ mm. \end{aligned}\right\} \quad (23)$$

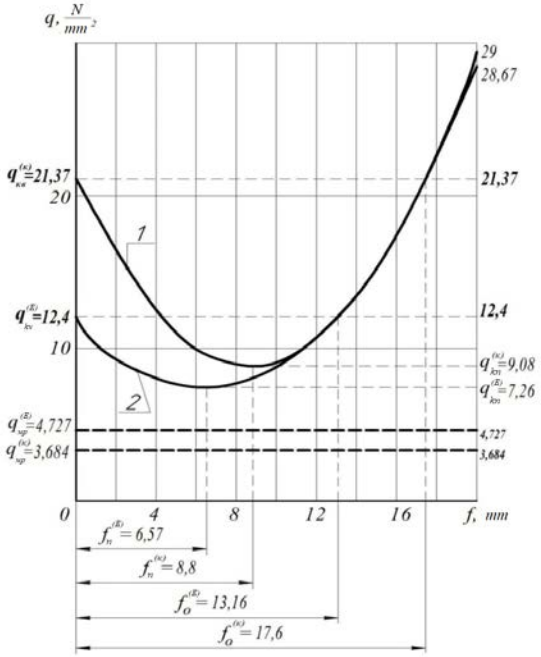

1 – Function $q^{(к)} = q^{(к)}(f)$ for round shell (20)
2 – Function $q^{(E)} = q^{(E)}(f)$ for elliptical shell (21)

Fig.2. Diagrams of "load-deflection" corresponding to the modified-modified functional relationships (20) and (21)

It is also marked by dotted thickened lines and the maximum possible operational extremes.

$$q_{мр}^{(к)} = 3{,}684\ \frac{N}{mm^2} = max, q_{мр}^{(E)} = 4{,}727\ \frac{N}{mm^2} \quad (24)$$

To improve the accuracy of the graphic display, the deflections are also shown in Fig. 7

$$f_0^{(к)} = 2f_n^{(к)} = 17{,}6\ mm, f_0^{(E)} = 2f_n^{(E)} = 13{,}16\ mm \quad (25)$$

under which identities are respected:

$$q^{(к)}(17{,}6) = q_{kv}^{(к)} = 21{,}37\ \frac{N}{mm^2}, q^{(E)}(13{,}26) = q_{kv}^{(E)} = 12{,}4\ \frac{N}{mm^2} \quad (26)$$

It is necessary to perform a condition control check (Doudkin et al., 2019)

$$\sigma_{ox}^{(max)} = \sigma_{ox}(0) = \frac{q_{kv} \cdot \pi \cdot R_c}{\delta \cdot 2 \cdot E(\xi) \cdot \sqrt{1-\xi^2}} < \sigma_m \quad (27)$$

using formula with $x_1 = 0, f = 0,\ q = q_{kv}$ confirming the physical and mathematical correctness of the refined theoretical and theoretical scheme of the cylindrical shell (Figure 1), that is, its guaranteed subcritical elasticity (without plastic deformations) during the operation of the road roller:

– in case of $\xi = 0,\ E(0) = 1{,}5708$ (round shell shape)

$$\sigma_{ox}^{(к)}(0) = \frac{q_{kv}^{(к)} \cdot R_c}{\delta} = \frac{21{,}37 \cdot 600}{6{,}5} = \\ = 1972{,}6\frac{N}{mm^2} < \sigma_m = 2270\frac{N}{mm^2}] \qquad (28)$$

– when $\xi = \xi_p = 0{,}57,$ but $E(0{,}57) = 1{,}434$ (elliptical shape of the drum surface (Abdeev et al., 2011)

$$\sigma_{ox}^{(E)}(0) = \frac{q_{kv}^{(E)} \cdot 3{,}1416 \cdot R_c}{\delta \cdot 2 \cdot 1{,}434 \cdot \sqrt{1-(0{,}57)^2}} = \\ = \frac{12{,}4 \cdot 3{,}1416 \cdot 600}{6{,}5 \cdot 2 \cdot 1{,}434 \cdot 0{,}82164} = \\ = 1526\frac{N}{mm^2} < \sigma_m = 2270\frac{N}{mm^2}, \qquad (29)$$

whence it follows that the margin of safety of the shell for the yield strength σ_m (Doudkin et al., 2019) varies from 13.1% to 32.8%.

The complexity of the mechanical and mathematical study of local deformations of the steel shell of a roller of a road roller with variable geometry of the contact surface and its analytical study makes it advisable to use finite element analysis, for example, using the APM FEM software package for KOMPAS-3D V17.1.

Consider the results of the static calculation in KOMPAS, as well as the analysis of the stability of the elastic cylindrical shell and the results of the calculation of the natural frequencies and the change in the natural vibration forms of the thin-walled shell as a result of the machine FEM analysis according to the given data of the shell model given in Tables 2, 3 and 4.

It should be noted that when modeling in APM FEM, KOMPAS-3D objects must be fixed in order to prevent the free movement of the elastic shell along any of the six degrees of freedom as an absolutely rigid body.

Table 2. Information on loads, material parameters (Steel), and the results of the model breakdown into cells

№	Indicator	Value	№	Indicator	Value
1	Yield point [MPa]	235	10	Pressure: 1	700 N
2	Elastic modulus normal [MPa]	200000	11	Pressure: 2	700 N
3	Poisson's ratio	0.3	12	Pressure: 3	200 N
4	Density [kg / m3]	7800	13	Item type	4 nodal tetrahedra
5	Temperature coefficient of linear expansion [1 / C]	0.000012	14	Maximum length of the side of the element [mm]	4
6	Thermal Conductivity [W / (m * C)]	55	15	Maximum surface condensation ratio	1
7	Compressive Strength [MPa]	410	16	Dilution ratio in volume	1,5
8	Endurance Limit [MPa]	209	17	The number of finite elements	195019
9	Torsion endurance limit [MPa]	139	18	Number of nodes	64262

a) b)

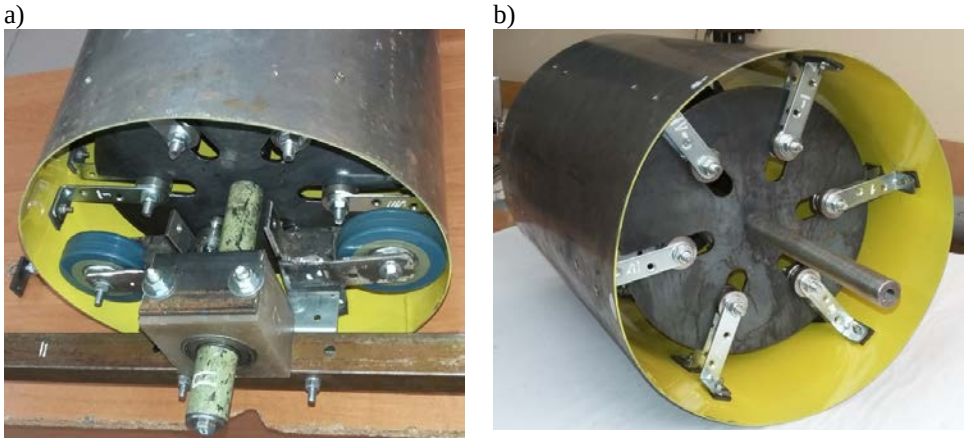

Fig. 3. Experimental model of a roller of a road roller with an elastic shell, capable of forcibly changing its shape: a) partial assembly without unclamping rollers; b) complete assembl

The boundary conditions are specified with regard to symmetry, according to which the points located in the cross section of the cylindrical shell, located at a distance of half the length of the cylinder from any of the ends, cannot move along the *z* axis. The points located on the end of the shell are prohibited to move in the *Oxy* plane. Points located on a circle lying in the plane of symmetry are not allowed to move along the *z* axis.

Further, to solve the problem, a grid with finite elements was built (Fig. 4). The results are contained in Tables 2 and 3, and are reflected in Figures 9-16.

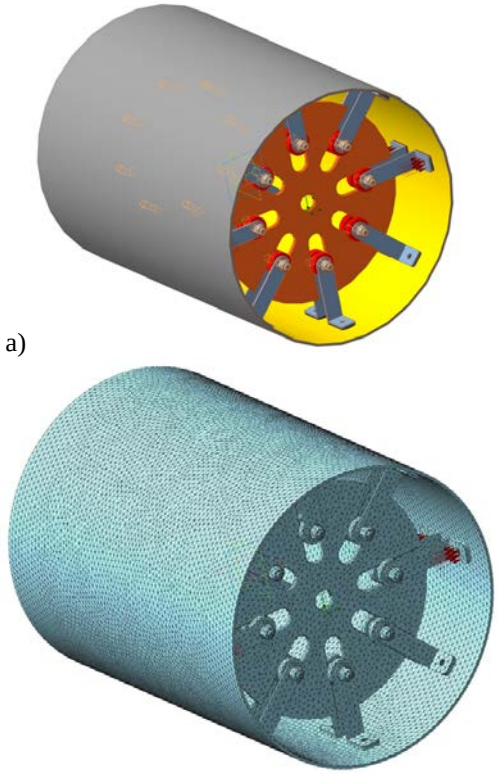

Fig. 4. Model of an elastic, thin-walled drum (a), divided into cells by a finite-element mesh (b)

Table 3. Inertial characteristics of the model

№	Indicator	Value
1	Mass of model [kg]	14.518466
2	Center of gravity of the model [m]	(-0 ; -0 ; -0.000002)
3	Moments of inertia of the model relative to the center of mass [kg * m2]	(0.566375 ; 0.392075 ; 0.392075)
4	Reactive moment relative to the center of mass [N * m]	(-0.000049 ; 0.000045 ; 0)
5	The total reaction of the supports [N]	(0 ; 0 ; -197.880822)
6	Absolute reaction value [H]	197.880822
7	Absolute moment value [N * m]	0.000066

Consider the results of static machine calculation in the figures.

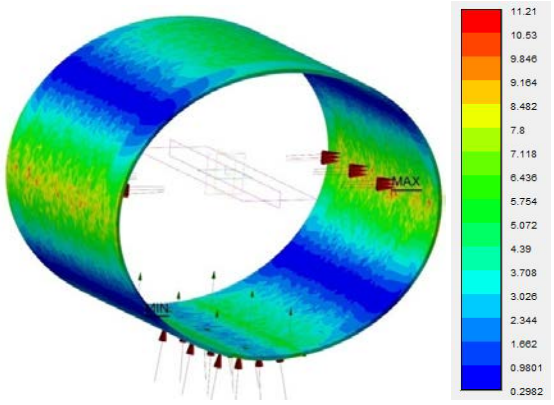

Fig. 5. Distribution of von Mises equivalent stresses

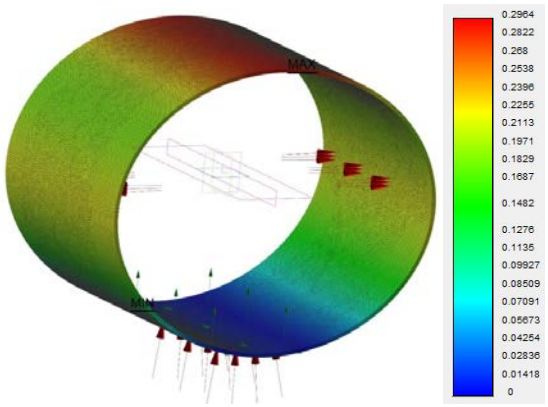

Fig. 6. Total linear displacement

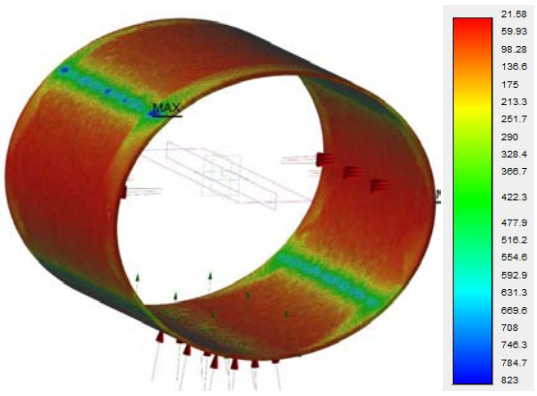

Fig. 7. Action on stress safety factor

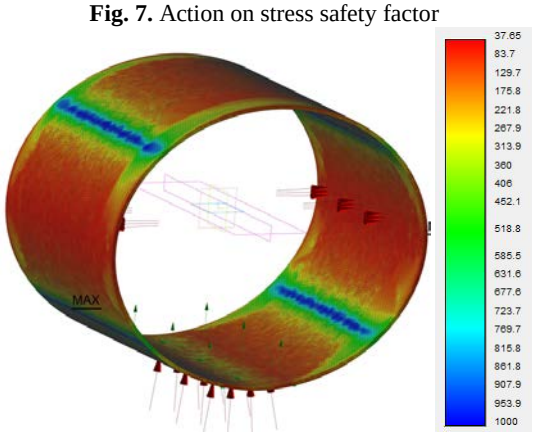

Fig. 8. Distribution of safety factor for strength

In the combined figures 9 - 13 the possible effect on the shell of natural frequencies is consider, divided into 5 ranges (Table 4).

Table 4. The results of the calculation of the natural frequencies of the shell

#	Frequency [rad/sec]	Frequency [Hz]
1	243.478794	38.750854
2	509.926404	81.157308
3	642.296838	102.224717
4	1432.696755	228.020771
5	1490.93104	237.289045

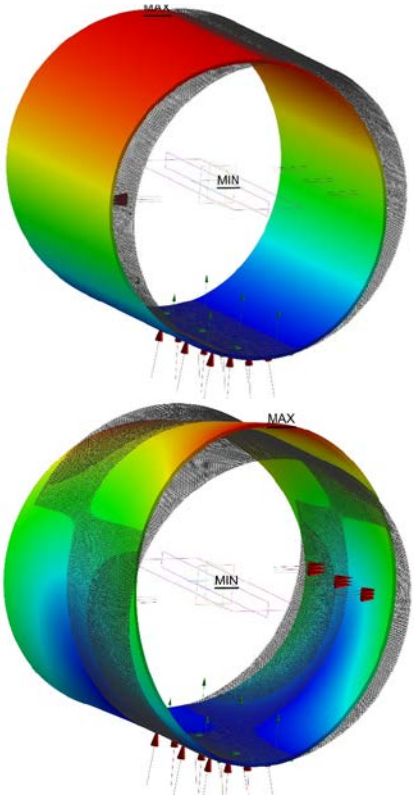

Fig. 9. 1st (a) and 2nd (b) forms of natural oscillations

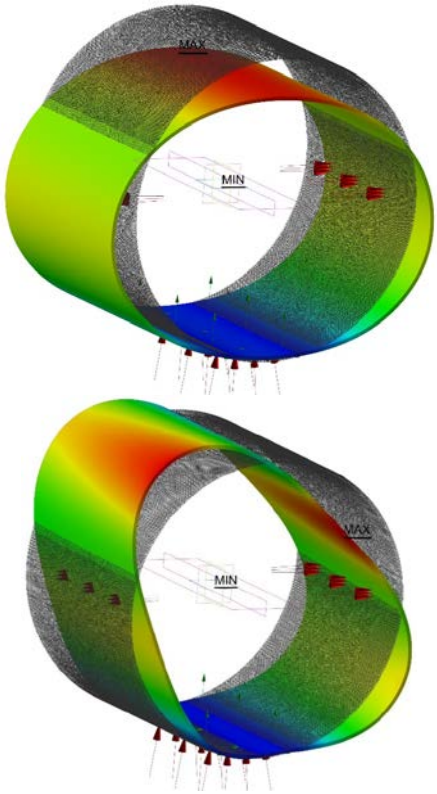

Fig. 10. 3rd (a) and 4th (b) forms of natural oscillations

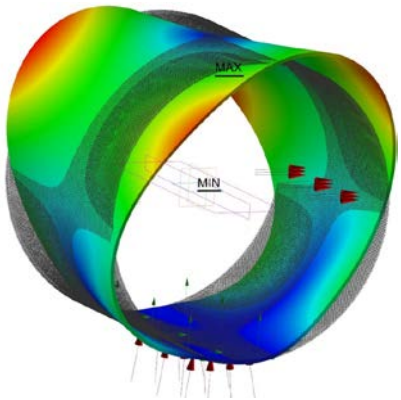

Fig. 11. 5th form of natural oscillations of the shell

The critical efforts obtained theoretically are several times larger than the values obtained using modeling in the APM FEM KOMPAS-3D, and, therefore, (as it happened) the results obtained using numerical analysis are much closer to the known experimental data than the theoretical results. This allows to conclude that a high degree of reliability of the results. This is explained by the fact that the theoretical model does not take into account, for example, the length of the elastic shell. When the grid is thickened 2 times, the critical efforts of the models obtained with the help of the APM FEM KOMPAS-3D, do not practically change. Also, the forms of buckling of a cylindrical elastic shell are almost unchanged.

The analysis of the tables and figures allows to conclude that the solutions obtained are close to the desired exact solution, since when the grid is thickened, the values of critical forces and forms of buckling, with the exception of some curvatures, for example, in 4 and 5 forms of natural oscillations of the shell, have changed.

3. Conclusion

The analysis of the research carried out allows the following conclusions to be drawn:

1) the Bubnov-Galarkin variational high-precision method solved in a first approximation the original nonlinear problem of the theory of elasticity and structural mechanics of machines by definition with a margin of bearing capacity of local deformations and stability of the steel shell of a roller of a road roller with varying geometry of the contact surface compacted until the residual displacements cease;

2) developed one-dimensional physical and mathematical models of cylindrical bending, clearly illustrated with characteristic numerical examples of a circular shell (K) and elliptical (E) outlines (Abdeev et al., 2011) (Fig. 2);

3) in the process of the performed calculations, it was proved that the considered elastic element with a thickness of 6.5 mm and a radius of 600 mm was deformed within the Hooke's law at stresses of not more than 86.9% of the yield strength $\sigma_{\text{т}}$= 2270 MPa ($\frac{N}{mm^2}$) steel grade 60C2XA (Abdeev et al., 2011) and theoretical safety factors $n_{\text{y}}^{(\text{к})}$ = 5,8 and

$n_y^{(E)}$=2,62 were much higher than the minimum acceptable value [n_y]=1,5 (Doudkin et al., 2019);

4) it was found that to prevent the occurrence of residual deformations, local dents and clicking (Kolkunov, 1972) of the shell, it is necessary to use only high-quality spring-spring steel with high $\sigma_т \geq$1800 MPa ($\frac{N}{mm^2}$) to make it, which is of great importance in this particular case - with high requirements for fatigue strength (Abdeev et al., 2011) and local resistance, corrosion and thermal resistance; in this regard, it is possible to recommend, for example, alloys on a cobalt-chromium-nickel base of the grades 40KXHM, 40KXHMBTU (GOST 10994-74) with $\sigma_т = 1800 \div 2500$ MPa ($\frac{N}{mm^2}$) and also some other special structural elastically deformable steels (60C2FA, 60C2XFA, 60C2XA, 65C2BA, etc.);

5) the results of mathematical modeling and FEM analysis make it possible to optimize the physical and geometric characteristics of the flexible shell during its design, thereby ensuring reliable operation of the roller with an adjustable outline of the working surface of the drum, economical consumption of expensive spring-spring steel and high-quality compaction of the road surface.

Reference

Abdeev, B.M., Dudkin, M.V., Sakimov, M.A., Eleukenov, M.T., 2011. *Applied theory of assessing the strength of the steel shell of the roller of a road roller with a change in the curvature of the cylindrical guide.* Vestnik D. Serikbaev EKSTU. - Ust-Kamenogorsk, 4/2011, 27-36 (Part 1), 1/2012, 35-45 (Part 2).

Birger, I.A., Shorr, B.F., Iosilevich, G.B., 1979. *Calculation of the strength of machine parts: a Handbook*, M.: Mashinostroenie, 702.

Bostanov, B.O., Temirbekov, E.S., Dudkin, M.V., Kim, A., 2018. *Mechanics-Mathematical Model of Conjugation of a Part of a Trajectory with Conditions of Continuity, Touch and Smoothness*, International Conference on Computer Aided Engineering, Computational and Information Technologies in Science, Engineering and Education, 9th International Conference, CITech, Ust-Kamenogorsk, Kazakhstan, Proceedings, 71-81, https://doi.org/10.1007/978-3-030-12203-4_8.

Doudkin, M.V., Kim, A., Kim, V., 2019. *Application of FEM Method for Modeling and Strength Analysis of FEED Elements of Vibroscreen*, Proceedings of the 14th International Scientific Conference on Computer Aided Engineering, June 2018, Series: Lecture Notes in Mechanical Engineering, Wroclaw, Poland, 892.

Doudkin, M.V., Kim, A., Kim, V., Mlynczak, M., Kustarev, G., 2018. *Computer Modeling Application for Analysis of Stress-strain State of Vibroscreen Feed Elements by Finite Elements Method*, Mathematical Modeling of Technological Processes International Conference, CITech 2018, Ust-Kamenogorsk, Kazakhstan, September 25-28, Proceedings, 82-96, https://doi.org/10.1007/978-3-030-12203-4_9.

Doudkin, M.V., Pichugin, S.Yu., Fadeev, S.N., 2013. *Studying the Machines for Road Maintenance*, Life Science Journal, 10(12), 134-138, doi:10.7537/marslsj1012s13.24.

Doudkin, M.V., Pichugin, S.Yu., Fadeev, S.N., 2013. *Contact Force Calculation of the Machine Operational Point*, Life Science Journal, 10(10), 246-250, doi:10.7537/marslsj1010s13.39.

Doudkin, M.V., Vavilov, A.V., Pichugin, S.Yu., Fadeev, S.N., 2013. *Calculation of the Interaction of Working Body of Road Machine with the Surface*, Life Science Journal; 10(12), 832-837, doi:10.7537/marslsj1012s13.133.

Dudkin, M.V., Kuznetsov, P.S., Sakimov, M.A., Golovin, A.A., Kiyalbaev, A.K., 2006. *Roller of road roller*, Provisional Patent RK 18131. A.S. Of the Republic of Kazakhstan, 51084, IPC E01C 19/26, EO1C 19/23. Publ. No. 12, December 15.

http://nblib.library.kz/elib/library.kz/jurnal/Геология_03_2018/Sakimov%20(str.207)%20032018.pdf

Kolkunov, N.V., 1972. *Fundamentals of the calculation of elastic shells*, M.: Publishing house "High School", 296.

Ponomarev, S.D., Andreeva, L.E., 1980. T*he calculation of the elastic elements of machines and devices*, M.: Mashinostroenie, 326.

Sakimov, M.A., Ozhikenova, A.K., Abdeyev, B.M., Dudkin, M.V., Ozhiken, A.K., Azamatkyzy, S., 2018. *Finding allowable deformation of the road roller shell with variable curvature*, News of the national academy of sciences of the republic of Kazakhstan series of geology and technical sciences, 3(429), 197-207.

Temirbekov, E.S., Bostanov, B.O., Dudkin, M.V., Kaimov, S.T., Kaimov, A.T., 2019. *Combined Trajectory of Continuous Curvature*, Advances in Italian Mechanism Science. Proceedings of the Second International Conference of IFToMM Italy, Mechanisms and Machine Science (MMS 68), 68, IFToMM ITALY, 12-19, https://doi.org/10.1007/978-3-030-03320-0_2.

接触面几何形状变化的压路机钢辊变形的数学和实验研究

關鍵詞

贝壳，
压路机，
鼓，
钢，
强调

摘要

缺乏压实理论的通用方法会刺激道路施工设备的开发人员创建各种近似的计算方法，目前，其数量可与拟议的压路机设计术语相提并论。

该文章介绍了在压路机的刚性圆形外壳被强制变形的椭圆形代替的情况下，对压路机的可变形壳行为及其压实辊下的压实材料的分析，该椭圆形不同于圆形设计

可以改变，调节和优化压路机对要压实材料的冲击。